GEOPHYSICAL RESEARCH LETTERS

Supporting Information for

Revisiting global vegetation controls using multi-layer soil moisture

Wantong Li[1*], Mirco Migliavacca[1], Matthias Forkel[2], Sophia Walther[1], Markus Reichstein[1] and René Orth[1]

[1]Department of Biogeochemical Integration, Max Planck Institute for Biogeochemistry, D-07745 Jena, Germany.

[2]Technische Universität Dresden, Institute of Photogrammetry and Remote Sensing, Helmholtzstr. 10, D-01069 Dresden, Germany.

*Corresponding author: Wantong Li (wantong@bgc-jena.mpg.de)

Contents of this file

Text S1. ERA5 Soil Moisture Evaluation

While the ERA5 soil moisture product is in principle derived with a land surface model and therefore can potentially reflect its shortcomings. The assimilation of observations from space-borne microwave instruments provides quantitative information for the surface SM, facilitating the retrieval of root-zone SM (Albergel et al., 2012). The model structure and parameterization governing the root-zone soil moisture dynamics has been thoroughly validated against related variables such as runoff or the surface heat fluxes (Balsamo et al. 2009, Balsamo et al. 2015). Therefore, we chose to use ERA5 multi-layer soil moisture in our analysis, even though it is necessarily less constrained by direct observations and larger uncertainties are expected for deep soil layers than for surface layers (Drusch et al., 2009).

Many studies evaluated soil moisture products from the European Centre for Medium-Range Weather Forecasts (ECMWF) (e.g. ERA5, ERA-Interim) against in-situ observations from global hydrology networks (Albergel et al., 2012; Albergel et al., 2013; Liu et al., 2013; Jing et al., 2018; Albergel et al., 2018; Li et al., 2020b; Hersbach et al., 2020). As listed above, most comparisons of reanalysis SM products agreed that ERA-Interim from ECMWF reproduces well the spatial and temporal dynamics, and ERA5 as the newest released product from ECMWF clearly enhances the simulation performance over ERA-Interim by improving the data assimilation from higher resolutions and better understanding the global balance of precipitation and evaporation.

Different layers of SM were also evaluated separately from the top down to 1 meter in many studies. Li et al., 2020b found that ERA5 total SM shows a higher consistency with observations than the other products at the network scale, while MERRA-2 is closer to the observations regarding to linear trends. Based on the hydrology network in Australia, Jing et al., 2018 evaluated first three layers in ERA-Interim SM, and concluded that all the evaluated layers of SM can capture temporal features well except for the depth of 28-100 cm in the winter, and the layer of 7-28 cm has higher absolute and temporal accuracy. Albergel et al., 2012 also evaluated the good quality of multi-layer SM from ERA-Interim even over 1 meter.

Text S2. More Details in the Random Forests (RF) Modeling

2.1. Cross-validation and Identification of Variable Importance Using RF

During RF model training, the data are randomly split 63% into training and the remaining into cross-validation when separating between decision trees, because bootstrap method is used in RF (Breiman 1996; Breiman 2001). After training, the performance of the RF model is evaluated at each 3x3 grid cell matrices by computing the R^2 between the modeled and observed target variable for data that was not used for training (out-of-bag data; Breiman 2001).

Permutation importance measures the relative importance of each predictor variable from the difference of errors before and after a temporal permutation applied to the particular variable (Cutler et al., 2012; Gómez-Ramírez et al., 2020). When RF perform regression, the difference of R^2 instead of errors is calculated, and the permutation importance generally ranges from -1 to 1, but a negative value indicates no efficient information from a predictor. To validate results of permutation importance we employ two more methods: (i) Spearman correlation (Zwillinger & Kokoska, 2000) and (ii) SHapley Additive exPlanations (SHAP) feature importance which measures marginal contribution of each predictor to the target variable (Lundberg et al. 2017; Sundararajan & Najmi, 2019).

2.2. SHapley Additive exPlanations (SHAP) Dependence to Measure the Target Sensitivity

In addition to the determination of the most relevant hydrometeorological controls we study the sensitivity of the vegetation response to each predictor variable. The sensitivity is determined by the slope from fitted linear quantile (median) regression between the SHAP dependence of a target variable and a predictor variable (similar method was applied by Forkel et al., 2019 using partial dependence plots), as SHAP dependence enables to measure the marginal effect each predictor variable has on the target variable for individual and global explanations (Lundberg et al. 2017). The magnitude and the sign of sensitivity complement the information in importance identification.

All data-processing and analyses are done with Python 3.7 by using the NumPy 1.16.1 (Oliphant 2006), Statsmodels 0.11.1 (Skipper & Perktold, 2010), Scikit-learn 0.22.1 (Pedregosa et al., 2011), Matplotlib (Hunter 2007) and shap 0.35.0 packages (Lundberg et al. 2017).

Text S3. Uncertainties in Vegetation Data and Model Tests

3.1. Uncertainties in Vegetation Data

NDVI can saturate because of red band reflectance in high biomass regions such as the Amazon, as it has been reported in previous studies (Huete et al., 1997; Huete et al., 2002). But a significant linear relationship between tower-based daily mean SIF and GPP has still been found even when NDVI clearly saturated at high GPP (Yang et al., 2015). In fact, unlike vegetation optical indices, SIF is mechanistically linked to photosynthesis, does not saturate in the tropics, and has been shown to have a near-linear relationship with ecosystem GPP at weekly and monthly scales (Guanter et al., 2012; Green et al., 2020). Magney et al., 2019 suggested that SIF is less affected by clouds and is not prone to saturate with high leaf area.

Dense canopy has the potential to confound the relationship between SIF and GPP, as the fluorescence escaping probability is associated with canopy structure (Fournier et al., 2012; Migliavacca et al., 2017; Dechant et al., 2020). However, Zeng et al 2019 and Dechant et al., 2020 show that SIF is highly sensitive to canopy structure that this underlies, in part, the strong correlation between SIF and GPP, particularly at the seasonal time scale. Besides, previous literature suggests that SIF and GPP could decouple under extreme environmental stresses due to leaf-level photosynthetic regulation (Helm et al., 2020; Wohlfahrt et al., 2018). In our analysis, we consider the full variability range of SIF conditions where extreme conditions only represent a small fraction of the data. We therefore expect that changing SIF-GPP relationship under extreme conditions do not have a major effect on our analyses.

Further, sun-sensor geometry could also confound SIF-GPP relationship, as Köhler et al., 2018 illustrated geometry effects in Amazon forests. While the differences accounting or not for the observation angle is not that much regarding to the correlation between SIF and GPP (He et al., 2017), and our study is focusing on partitioning global controls on vegetation productivity in global domain using half-month data anomalies, and thereby the influence of observation angles would not conclude to a different pattern of global vegetation controls with consistent main results coming from SIF, NIRv and NDVI.

3.2. Model Tests

We perform further RF model experiments to investigate if the added skill in the case of the multi-layer SM is related to the increased number of predictor variables, and therefore an increased flexibility of the model, or to the additional information contained in the individual layers compared with the total SM. First, the experiment of multi-layer RF (4 variables) preforms better than the experiment of 5 SM variables, showing that the enhanced performance is not exclusively due to the increased number of variables and hence increased flexibility of the RF model (Figure S3). We note that, the fifth layer is supposed to provide no additional information as a weighted average from the other four predictor variables it is. Second, regionally enhanced performance can be found when replacing total SM with individual layers (Figure S4), indicating that additional information can be explored by the RF model from SM from individual layers.

Text S4. Complemented analyses about main Hydrometeorological Controls on Sun-induced fluorescence (SIF)

4.1. Main Hydrometeorological Controls on Sun-induced fluorescence (SIF) When Only Considering Positive Variable Contributions

We repeat the analysis from Figure 2 while only considering variables with positive contributions to SIF prediction. The result shows that consistent proportions of water-related controls can be found when using multi-layer SM, while around 4% of the study area is shifted from energy- to water-control in the total SM experiment, confirming potential confounding effects can be minimized using multi-layer SM (Figure S6). However, total SM does not provide sufficient information to the RF model to detect water-controlled regions, because confounding effects may mislead main controls identification. For example, energy-related variables can misleadingly be detected as main controls in the total SM experiment in the case that surface soil moisture is the actual main driver: temperature and VPD co-vary with surface soil moisture, while its variations are overshadowed by that of deeper layers in the total SM information.

4.2. Main Hydrometeorological Controls on Sun-induced fluorescence (SIF) in the Early and Late Growing Seasons

The main hydrometeorological controls which we determine for the entire growing season may vary from early to later periods. To analyze potential differences, we separate the growing season into two periods, an early period before the first peak of the seasonal cycle of SIF (half-month with the highest SIF across each year) in each grid cell, and a later period including the peak and the time thereafter. In the early growing season, larger regions show temperature control, such as the north Europe, while in the late growing season, the control of root-zone soil moisture (7-28 cm in ERA5) is expanded, such as the central North America and south Europe (Figure S10). Despite the difference in could cover between the early and late growing season periods we find overall similar results but expected increased water controls following the drier conditions (Figure S10), highlighting that cloud cover likely has no major influence on our results. Elevated evapotranspiration in the early growing season can induce water deficits in the later growing season in previously energy-limited ecosystems, and hence soil moisture plays a more important role in vegetation productivity in the later growing season, especially in the transition zone of climate and vegetation types (Figure S11; Zhang et al., 2020; Buermann et al., 2018; Lian et al., 2020). Patterns for the whole growing season are generally consistent with these two partitioned periods (Figure 3a, d; Figure S10a). We note, however, that alternative approaches of distinguishing between early and late growing seasons can affect these results, especially for regions with complex growing season timing, even though the main conclusion with the increased water-control is expected to hold.

Text S5. Additional Global Soil Moisture and Rooting-depth Products

To further complement our results on the relative importance of vertical SM layers, we include three global model-based products of vegetation rooting depth distributions from (i) Fan et al., 2017 (https://wci.earth2observe.eu/thredds/catalog/usc/root-depth/catalog.html), (ii) Schenk & Jackson, 2009 (https://daac.ornl.gov/ISLSCP_II/guides/ecosystem_roots_1deg.html), and (iii) from Yang et al., 2016 (effective plant rooting depth, https://data.csiro.au/collections/collection/CI19813).

Rooting depths from Fan et al. 2017 and Schenk & Jackson, 2009 show similar patterns with deepest roots in semi-arid areas and for non-tree vegetation such as grasses and shrubs (Figure 4d-i). Less agreement is found with the rooting depths from Yang et al. 2016 (Figure S12). The former two products were rooting-depth data driven by extrapolation, and the one from Yang et al. 2016 was instead derived by a hydrological model by balancing the trade-offs between carbon costs and the benefits of deep rooting. From a perspective of maximum physical rooting depths modeling, actual effective water uptake may partly diverge inferred by the former two products due to ignored seasonal variability of hydraulic traits in the model framework, while the third one may largely underestimate effective roots in grasses, shrubs and savannas without using deep rooting strategies (Sakschewski et al., 2020).

To validate our findings we also use alternative SM products: (i) MERRA-2 surface and root-zone SM (Gelaro et al., 2017), (ii) GLEAM v3.3 surface and root-zone SM (Martens et al., 2017), and (iii) SoMo.ml with three layers (O and Orth, 2020). Table S1 shows the information of depths for all SM products that we use and classify into surface SM and root-zone SM.

	Surface SM	Root-zone SM
ERA5	Layer 1 (0-7 cm)	Layer 2 (7-28 cm)
		Layer 3 (28-100 cm)
		Layer 4 (100-289 cm)
GLEAM	Layer 1 (0-10 cm)	Layer 2 (10-100 cm)
MERRA-2	Layer 1 (0-5 cm)	Layer 2 (0-100 cm)
SoMo.ml	Layer 1 (0-10 cm)	Layer 2 (10-30 cm)
		Layer 3 (30-50 cm)

Table S1. Depths and layers for different soil moisture (SM) products

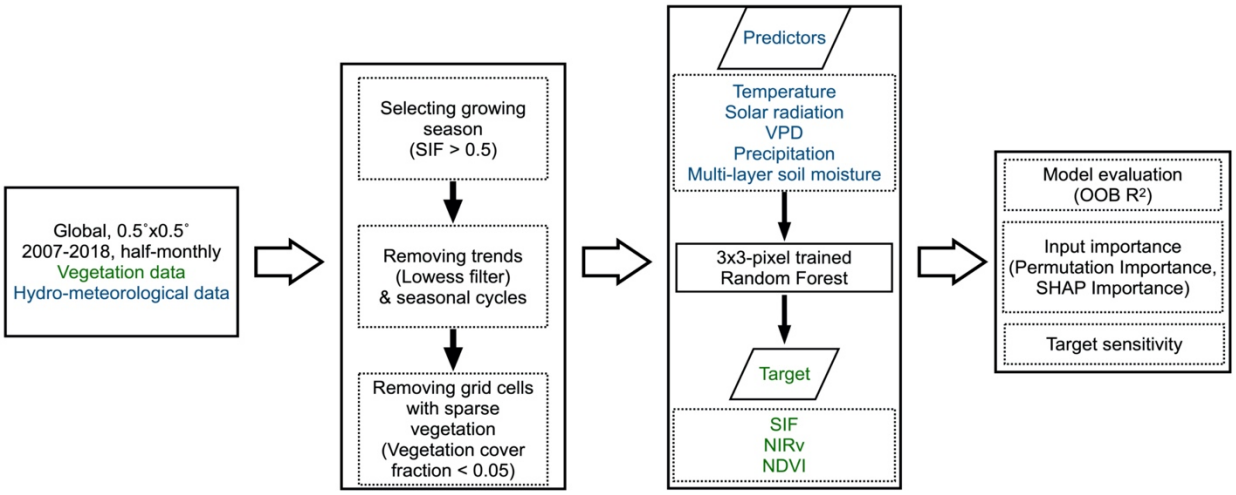

Figure S1. The flow chat of data-processing and data analysis. Details about data-processing can be found in the Data and Methods section. Hydrometeorological data are considered as predictor variables (blue color). Vegetation data relating to different proxies of vegetation productivity (normalized difference vegetation indices, NDVI; near-infrared reflectance vegetation, NIRv; and sun-induced fluorescence, SIF) are the target variable (green color). Three aspects are needed when implementing predictions: Model evaluation by Out-of-bag (OOB) R^2 is conducted to test our methodology. Permutation importance method is used to identify the relative importance of each predictor variable. SHapley Additive exPlanations (SHAP) importance method is also used to confirm the result of Permutation Importance. Target sensitivity is the slope of each linear regression between SHAP dependence and one predictor variable to obtain the sensitivities of target variables (e.g. SIF) to predictor variables (e.g. multi-layer SM).

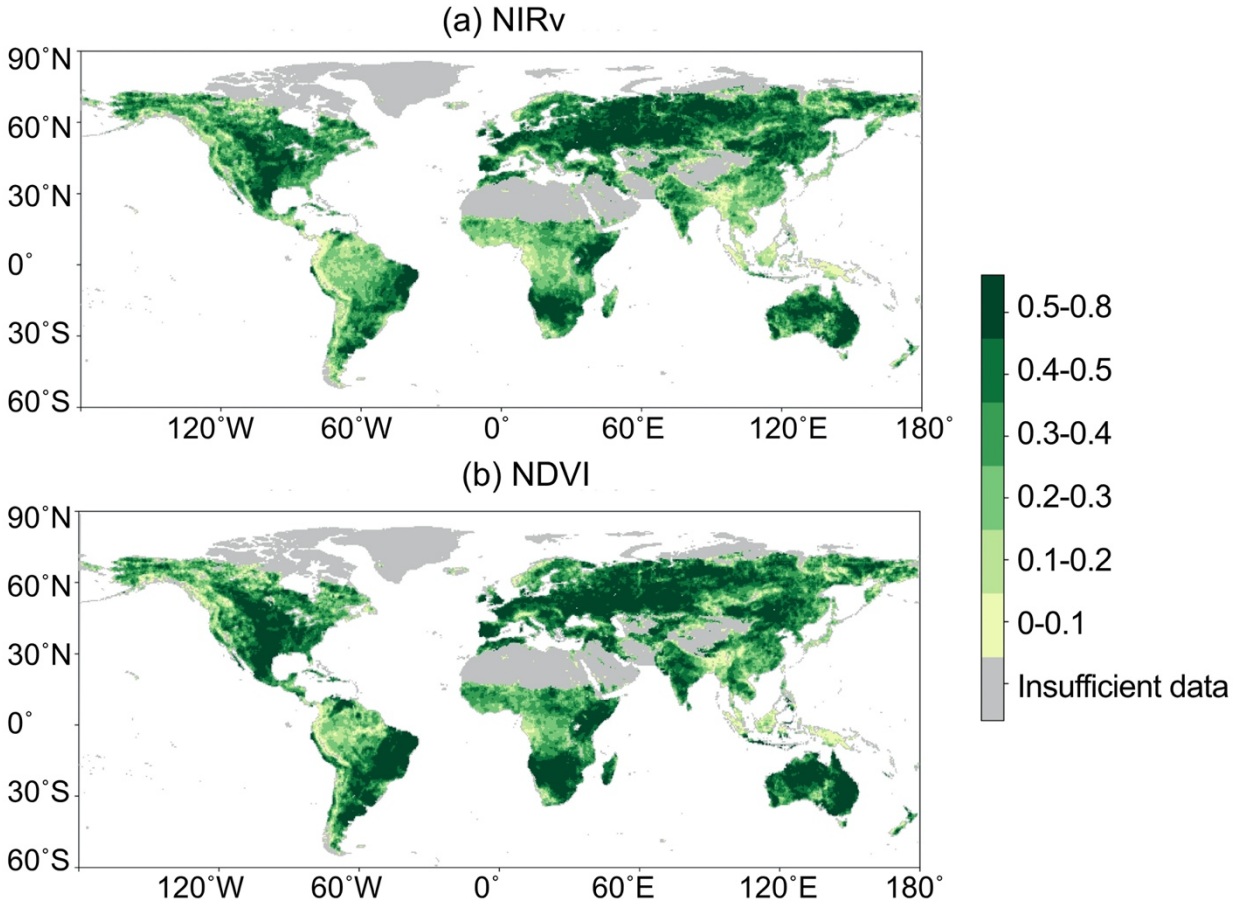

Figure S2. Model performance (R^2) in prediction for (a) NIRv and (b) NDVI in the multi-layer SM (SM layer 1, 2, 3 and 4) experiment.

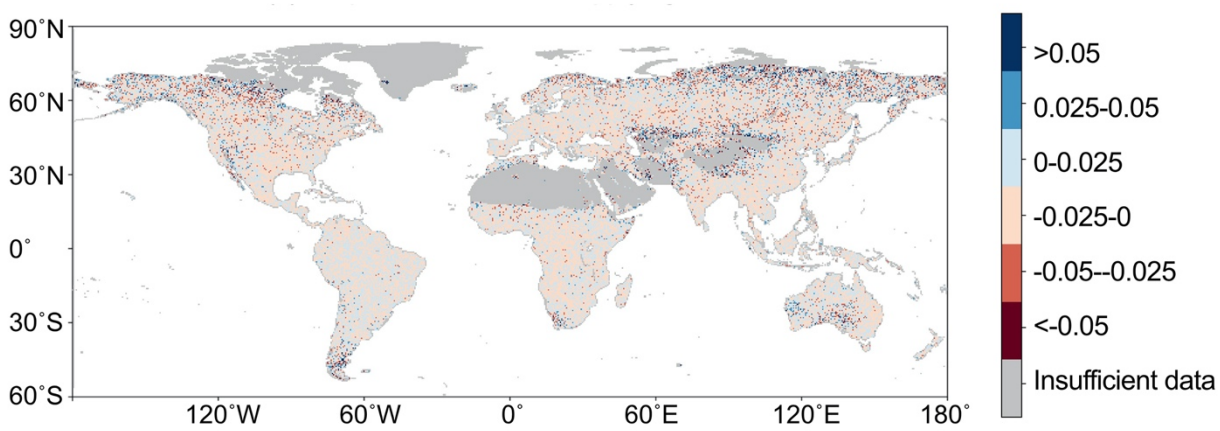

Figure S3. The differences of R^2 in predicting SIF between the experiments with 5 variables of SM (SM layer 1, 2, 3, 4, and total SM) and 4 variables of SM (SM layer 1, 2, 3, and 4) as predictors. The differences in prediction performance using 4 or 5 layers of SM are negligible, indicating that the increase in model performance when using 5 SM layers are not exclusively due to the increased number of variables and hence increased flexibility of the RF model.

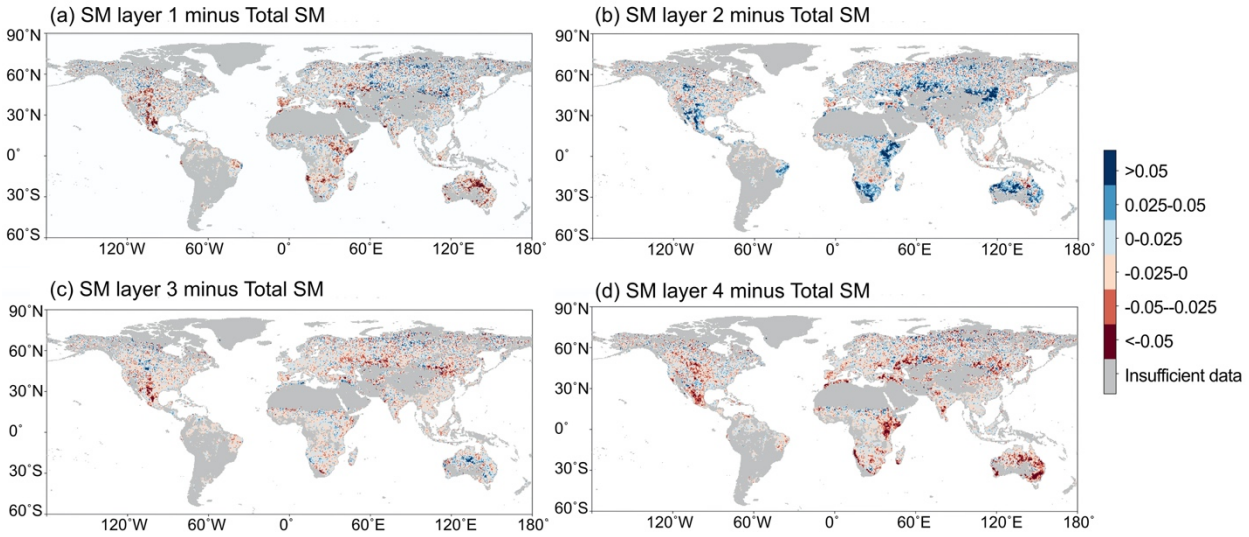

Figure S4. The differences of R^2 in predicting SIF between models including (a) SM layer 1, (b) SM layer 2, (c) SM layer 3, or (d) SM layer 4, with a model including total SM. All the other predictor variables (precipitation, temperature, solar radiation, and VPD) are used in the analyses as predictors. Regions with positive values show that the performance of SIF prediction using one individual SM layer as predictor is better than using total SM as predictor.

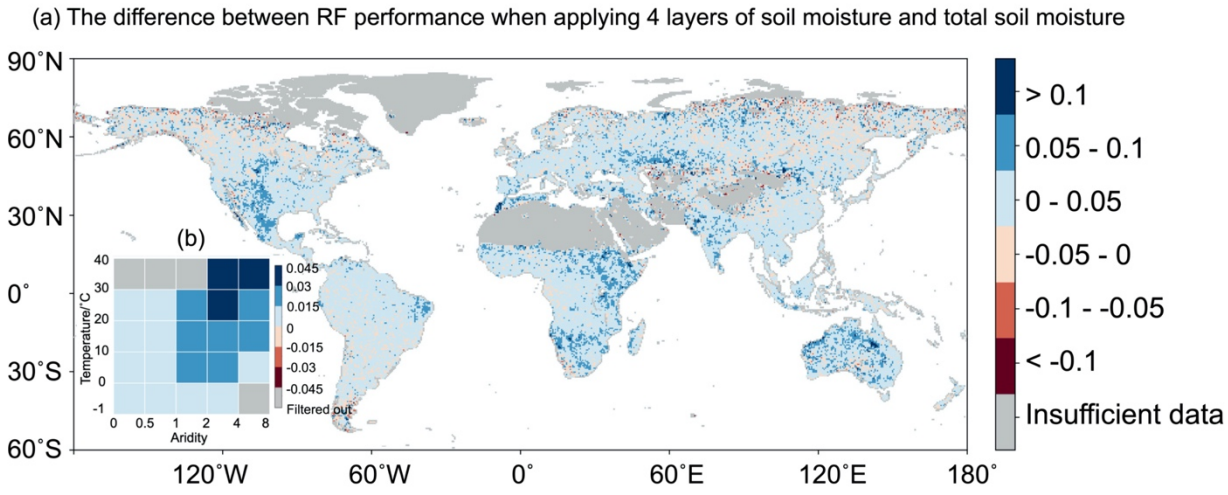

Figure S5. The differences of R^2 in predicting SIF between models including multi-layer soil moisture and total soil moisture, and (b) summarizes differences across climate regimes. Figure S5 a is similar to Figure 1 c but total soil moisture is calculated by 4-layer averages weighted by root fraction per layer from ERA5 scheme.

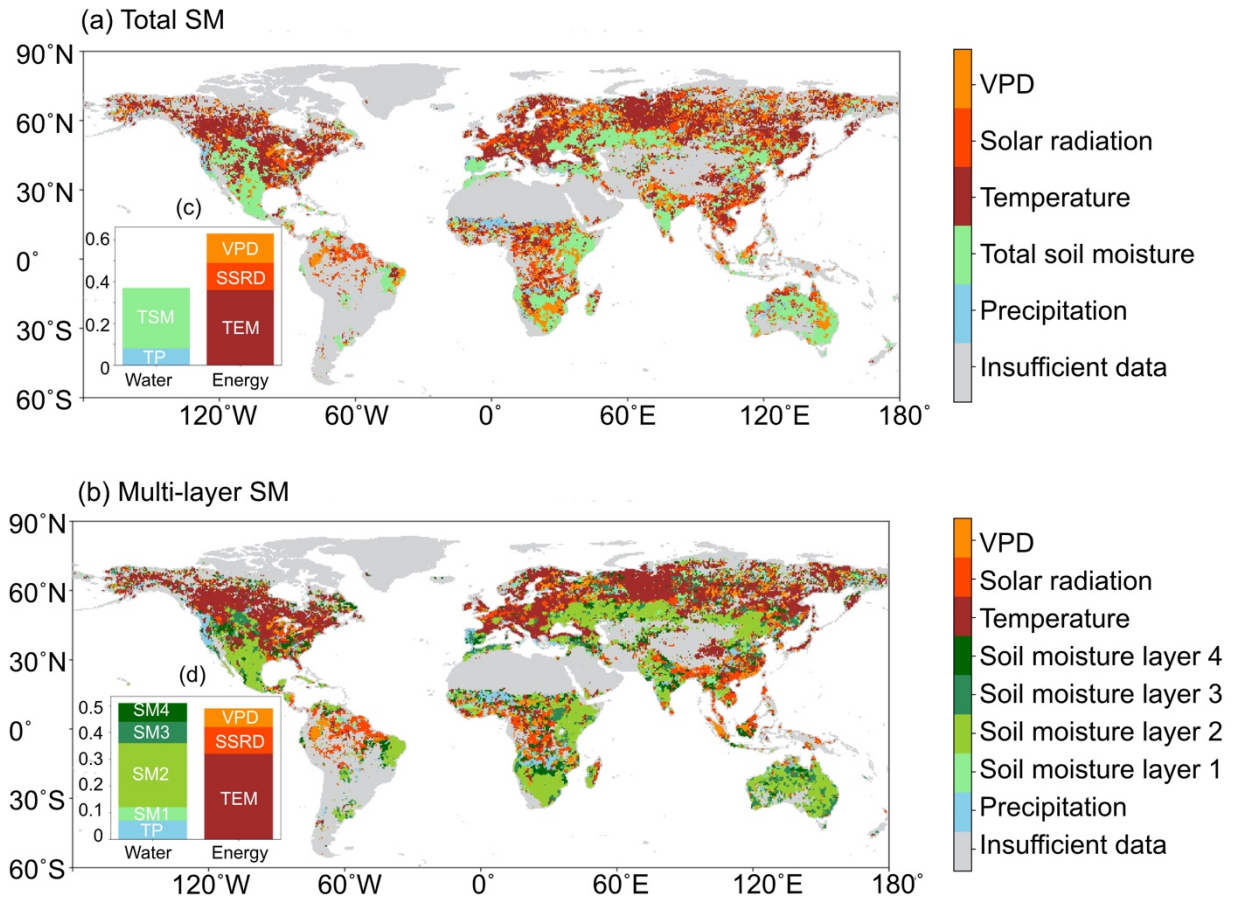

Figure S6. Main hydrometeorological controls on sun-induced fluorescence (SIF) by only considering grid cells and variables with positive contributions using (a) total soil moisture (SM) alongside all other predictor variables, and (b) multi-layer SM alongside all other predictor variables. The figure insets (c and d) representing the proportion of study area where each variable is the most important factor. Figure S5 is similar to Figure 2 but focusing on positive contributions from hydrometeorological variables only.

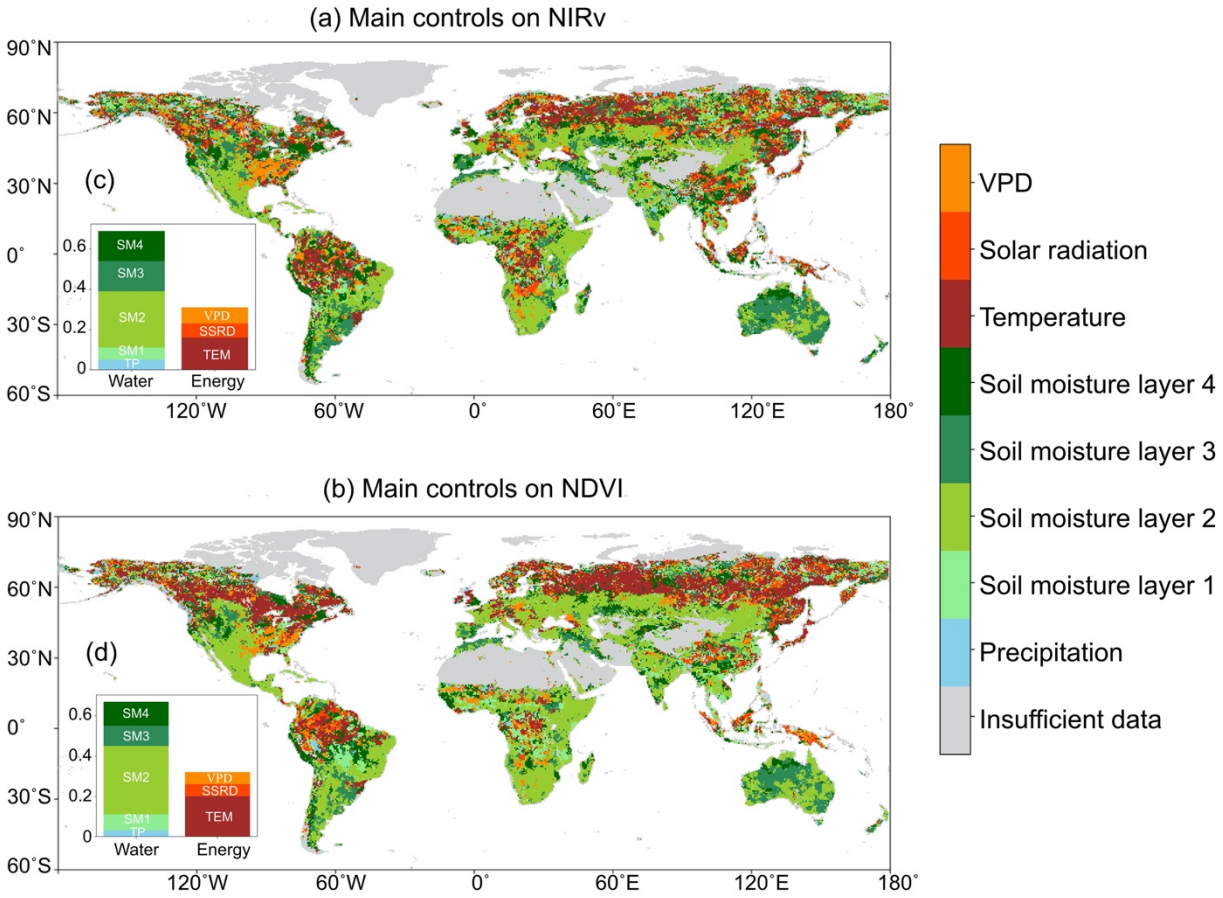

Figure S7. Main hydrometeorological controls on (a) NIRv and (b) NDVI at a global. The figure insets (c and d) representing the proportion of study area where each variable is the most important factor.

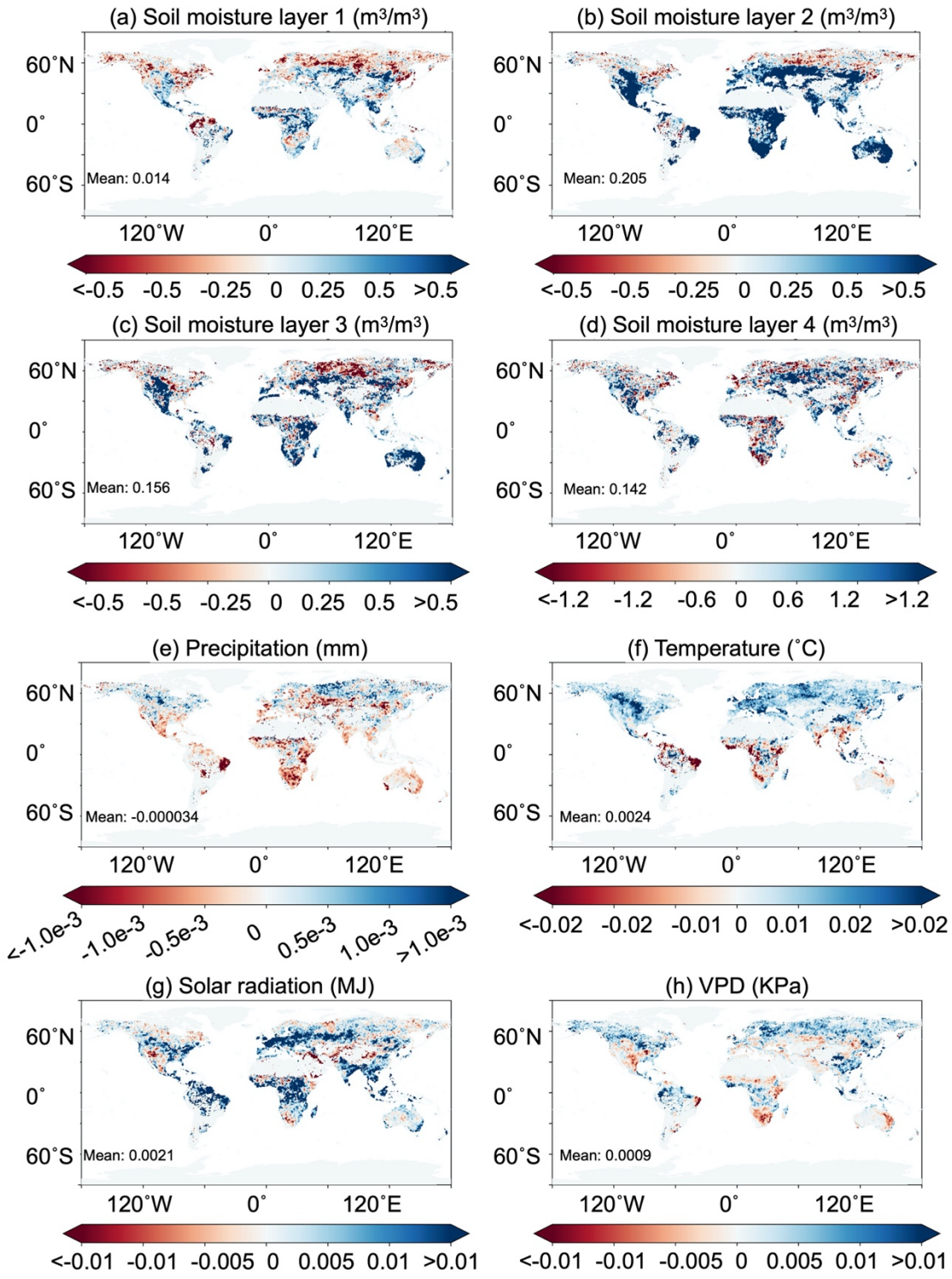

Figure S8. The sensitivities of SIF to hydrometeorological controls at a global scale. Mean values are calculated for all grid-cells in the map except the ones with fractional vegetation cover below 5% and poor performance in SIF prediction (R^2<0).

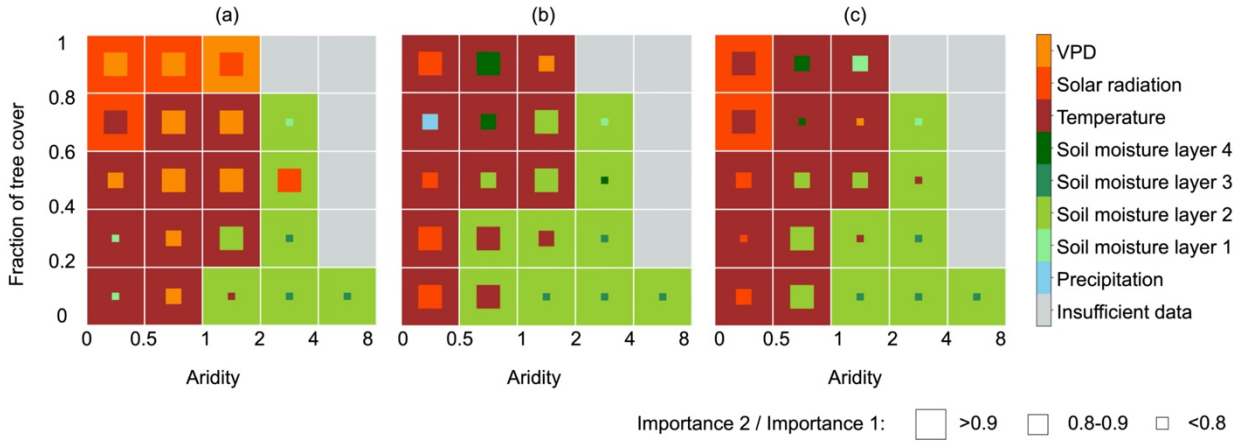

Figure S9. Main hydrometeorological controls on (a) SIF, (b) NIRv, and (c) NDVI across classes of fraction of tree covers and aridity.

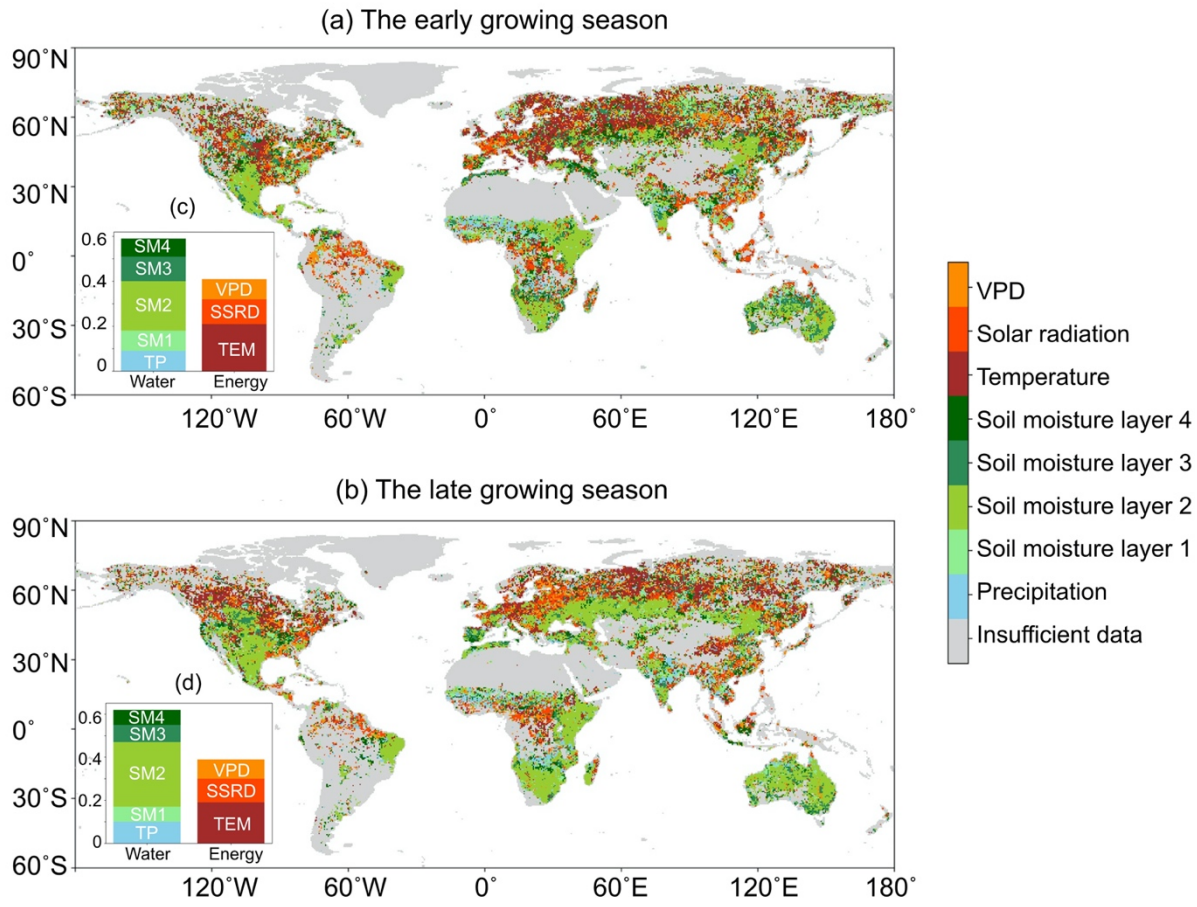

Figure S10. Main hydrometeorological controls on sun-induced fluorescence (SIF) in the (a) early and (b) late growing seasons at a global. The figure insets (c and d) representing the proportion of study area where each variable is the most important controlling factor.

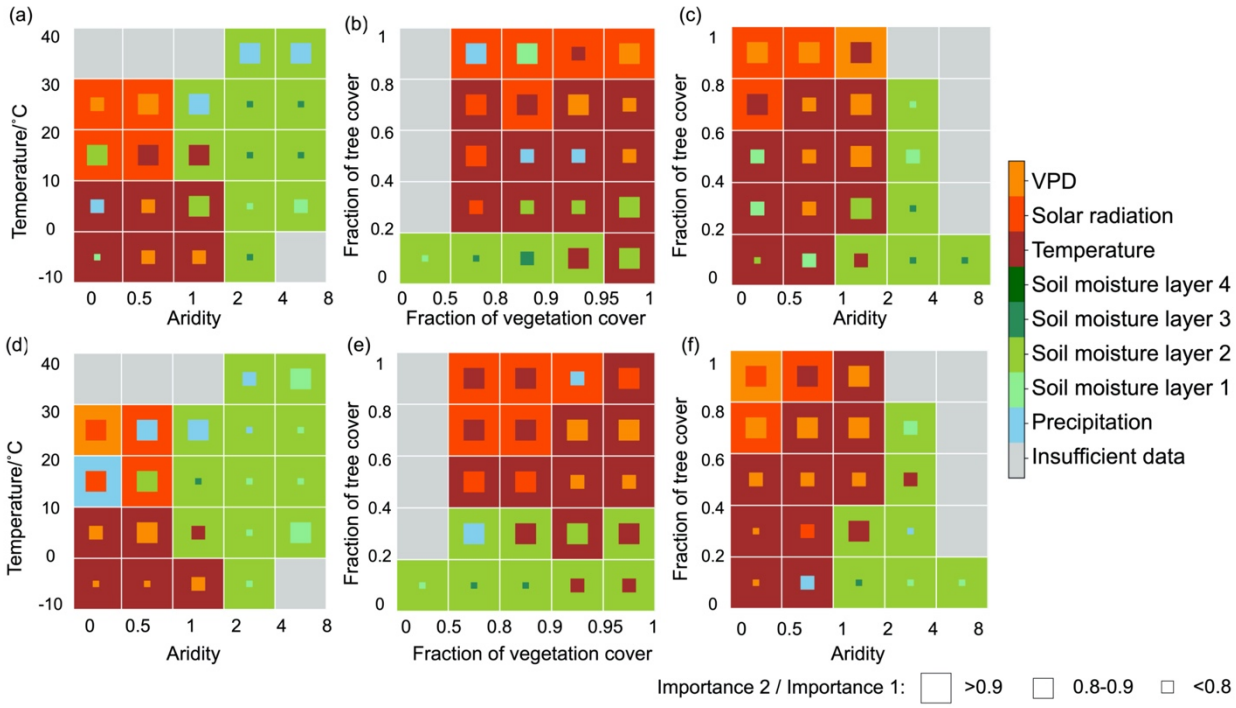

Figure S11. Main hydrometeorological controls on sun-induced fluorescence (SIF) in the (a, b, c) early and (d, e, f) late growing seasons across climate regimes, vegetation characteristics and classes of fraction of tree covers and aridity.

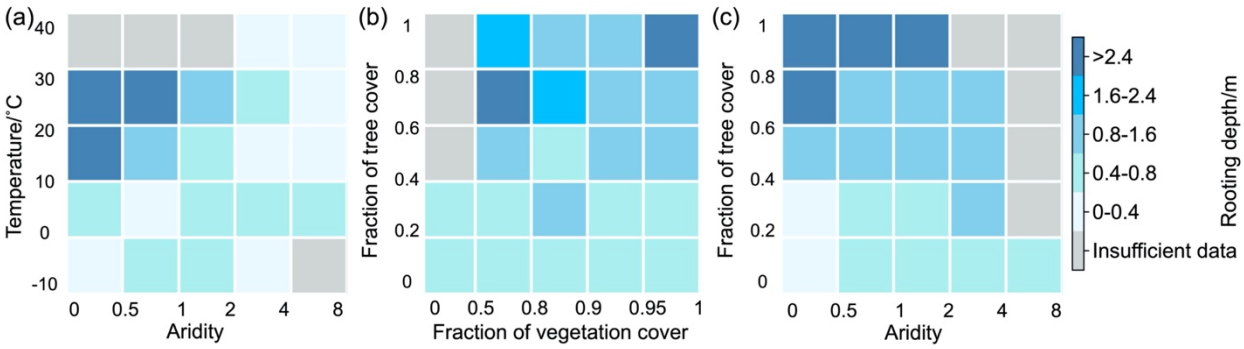

Figure S12. Distributions of rooting depths from Yang et al. 2016 across (a) climate regimes, (b) vegetation characteristics, and (c) classes of fraction of tree covers and aridity.

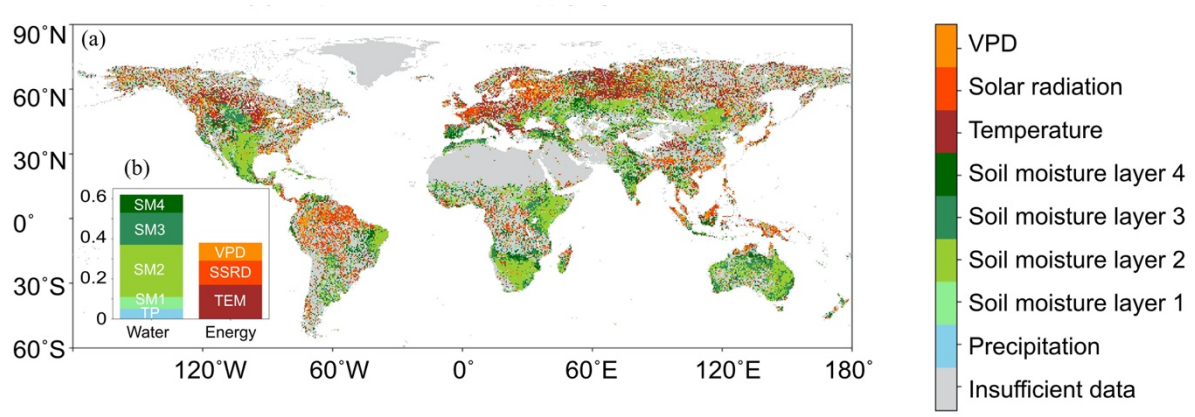

Figure S13. Main hydrometeorological controls on SIF by applying Spearman Correlation (a) in a global scale and (b) with proportion of study area where each variable is the most important factor.

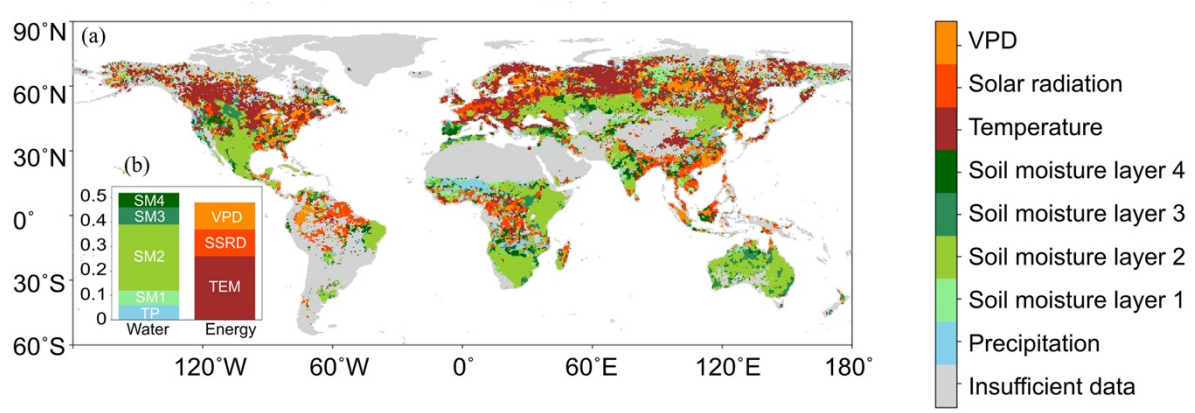

Figure S14. Main hydrometeorological controls on SIF by applying SHAP feature importance method (a) at a global scale and (b) with proportion of study area where each variable is the most important factor.

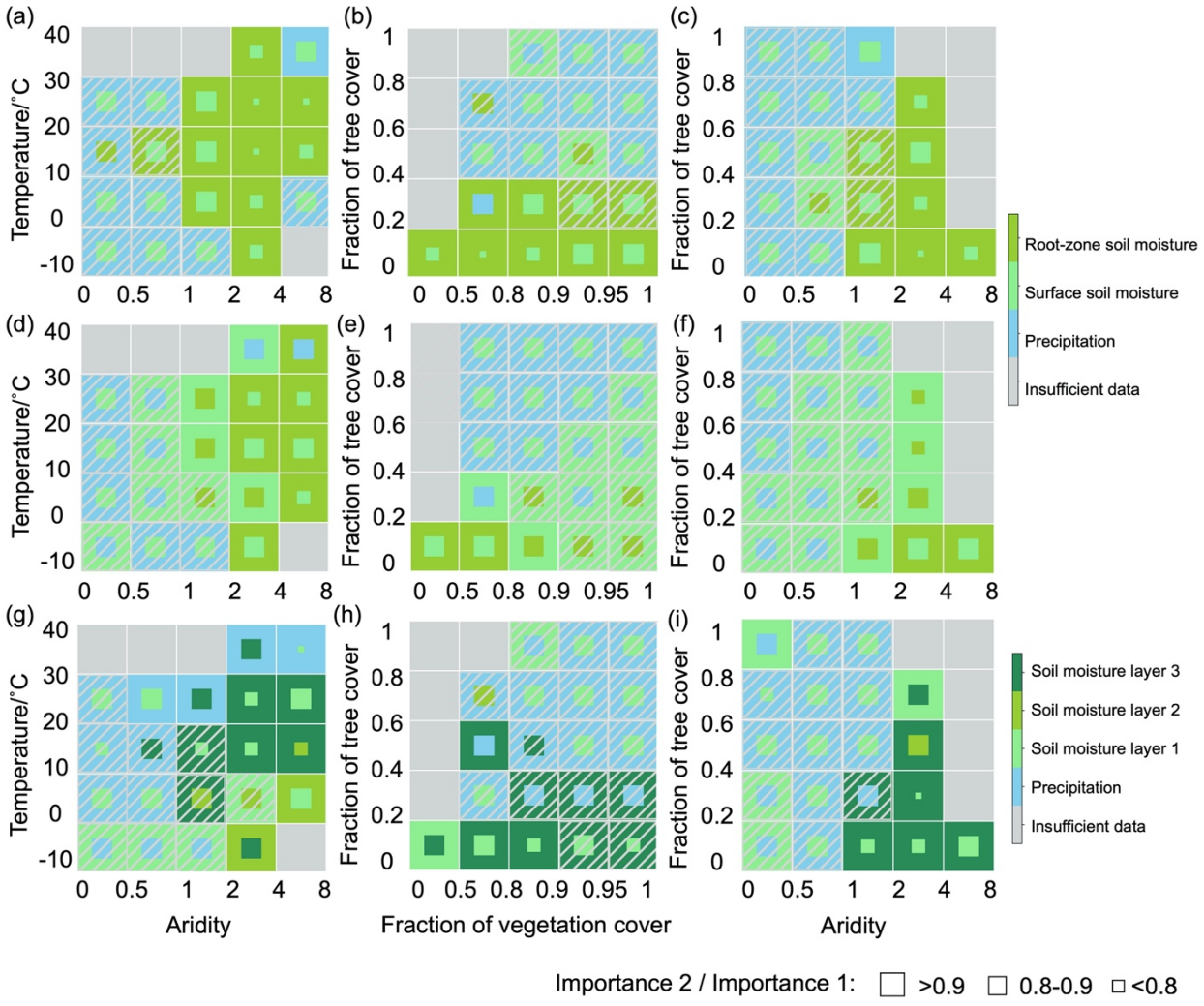

Figure S15. Main water-supply-related controls on SIF by applying (a-c) GLEAM soil moisture, (d-f) MERRA-2 soil moisture and (g-i) SoMo.ml across climate regimes, vegetation characteristics and classes of fraction of tree covers and aridity. Dark-gray hatching indicates that temperature, solar radiation or VPD is identified as the main control on SIF in these boxes.

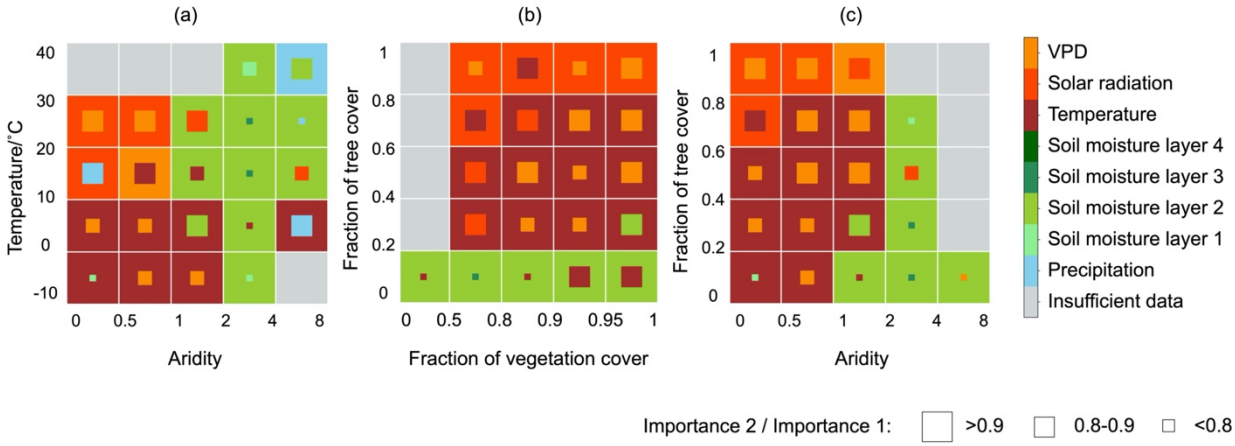

Figure S16. Main hydrometeorological controls on SIF using water potentials across (a) climate regimes, (b) vegetation characteristics, and (c) classes of fraction of tree covers and aridity. Water potentials in ERA5 scheme are calculated by the differences between actual volumetric soil moisture and volumetric soil moisture in permanent wilting point defined by the soil type per grid cell from ERA5 scheme.